



The synthesis and deep purification of GaEt₃. Reversible complexation of adducts MAlk₃ (M = Al, Ga, In; Alk = Me, Et) with phenylphosphines

V.V. Shatunov^{a,*}, A.A. Korlyukov^{b,1}, A.V. Lebedev^a, V.D. Sheludyakov^a, B.I. Kozyrkin^{c,2}, V.Yu. Orlov^{c,2}

^aState Scientific Center RF GNIICHTEOS, 38, shosse Entuziastov, Moscow 111123, Russia

^bA.N. Nesmeyanov Institute of Organoelement Compounds, Russian Academy of Sciences, Vavilova str. 28, 119991, Moscow, Russia

^cJSC Alkyl, d. 3, str. 1, proezd 4807, Zelenograd, Moscow, 124489, Russia

ARTICLE INFO

Article history:

Received 6 July 2010

Received in revised form

1 November 2010

Accepted 28 November 2010

Keywords:

Gallium trialkyls

Aluminum trialkyls

Indium trialkyls

Triphenylphosphine

Bis(diphenylphosphine)alkanes

Synthesis

ABSTRACT

Optimal parameters of organomagnesium technique of synthesis of triethylgallium have been defined. Various techniques of deep purification of triethylgallium to the extent required in metalorganic vapor-phase epitaxy MOVPE have been studied: by way of residue ether displacement through high-performance rectification and interaction with high pure aluminum and gallium trichloride, and by way of reversible complexation with triphenylphosphine, 1,3-bis(diphenylphosphine)propane and 1,5-bis(diphenylphosphine)pentane. Advantages and disadvantages of each technique have been identified. We have shown high performance of adduct purification technique covering trimethyl and triethyl derivatives of aluminum, gallium and indium. The structure of donor–acceptor complexes between metal alkyls and the above-mentioned phosphines have been verified using H and ³¹P NMR spectroscopy and X-ray studies, as well as quantum chemical calculations. Thermal stability of triethylgallium and oxidation of its adducts with phosphines have been studied.

© 2010 Elsevier B.V. All rights reserved.

1. Introduction

Several techniques are used nowadays for epitaxial growth of semiconductors: liquid-phase epitaxy, chloride vapor-phase epitaxy, hydride vapor-phase epitaxy, molecular beam epitaxy and metalorganic vapor-phase epitaxy (MOVPE). Each technique has its advantages and disadvantages [1,2]. The MOVPE technique is usually considered as one of the most progressive techniques for the growth of compound semiconductors containing the Group 13 elements, such as Al, Ga and In, due to intensified researches aimed at producing ultrapure precursors to grow epitaxial layers. Consequently, requirements for high purity organometallic compounds of MR₃ (M = Al, Ga, In) type have become much tighter, because they can be widely used in production of semiconductor devices. A commercial use of alkyl derivatives of the above metals in MOVPE makes it possible to grow two-component (GaN, GaAs), three-component (AlGaAs, InGaAs, InGaP) and four-component (AlGaInP, AlGaInAs) epitaxial structures. These structures are used in production of broadband light-emitting diodes, solid-state

lasers, solar cells, optical sensors, microwave devices, optical fiber and other devices. However, due to difficulties in production of high purity Al, Ga and In trialkyl compounds their use in MOVPE processes is restricted by high production cost and low availability of those organometallic precursors.

An adduct purification technique has been applied to purify the Group 13 trialkyls [3–8]. This involves the formation of an involatile Group 13-Lewis base adduct from which volatile non-adducting, or weakly adducting impurities (e.g. R₄Sn, R₄Si, R₂Zn) can be removed by vacuum distillation. The adduct is then thermally dissociated at moderate temperatures to liberate the purified Group 13 trialkyl. An adduct purification technique has been known for a long time and used to purify trimethylgallium using high-boiling ethers (i-Am)₂O and Bu₂O [9,10], amines [11] and phosphines [11,12].

Hence, it seemed reasonable to develop optimal production techniques for alkyl derivatives of aluminum, gallium and indium. The purpose of this research, the results of which are described below, has been to develop an optimal synthesis technique for high purity triethylgallium being in the highest demand and effective chemical purification techniques for methyl and ethyl derivatives of Al, Ga and In.

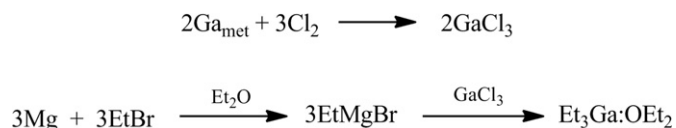
2. Results and discussion

The analysis of literature concerning synthesis techniques for gallium trialkyls [13] has shown that one of the most effective

* Corresponding author. Tel.: +7 905 717 8341; fax: +7 495 673 7124.
E-mail addresses: vdsh2004@yandex.ru (V.V. Shatunov), alex@xrlab.ineos.ac.ru (A.A. Korlyukov).

¹ Fax: +7 499 135 5085.

² Fax: +7 499 734 3765. elmos@mail.ru

**Scheme 1.** GaEt₃ synthesis using Grignard reagent.

techniques of their production is organomagnesium one. We have established that the high-efficiency synthesis technique for Et₃Ga can be applied as follows: metal Ga is chlorinated to GaCl₃ which is processed then with a Grignard reagent in diethyl ether by the following scheme (Scheme 1).

The gallium melt interacts with gaseous chlorine to produce GaCl₃ with yield of 99%. The content of trace impurities in GaCl₃ has been determined using ICP spectroscopy and presented in Table 1. The direct chlorination is far more effective than the impact of dry purified gaseous HCl on metal gallium due to less strict requirements to corrosion resistance of the equipment used.

The reaction of gallium trichloride with Grignard reagents gives the highest yields with diethyl ether used as a solvent. Ethyl magnesium bromide has been selected out of Grignard reagents. It has been experimentally determined that the optimal mole ratio EtMgBr/GaCl₃ is 3.4. As Table 2 shows, such ratio of the reagents results into the highest GaEt₃ yield. The product has been isolated using fractional distillation. The lower is the mole ratio EtMgBr/GaCl₃, the lower is GaEt₃ yield. It is not reasonable to increase the mole ratio, because it does not improve a yield of the end product. The set optimal ratio of reagents can be apparently explained by the fact that the first stage of the process, i.e. preparation of Grignard reagents, gives a yield of ca. 90% because of the previously reported secondary processes.

Based on ¹H NMR results GaEt₃ obtained contains 4–5% w/w of diethyl ether as is verified by a quadruplet signal of O–CH₂ fragments at δ equal to 4.09 ppm. The signals of methylene groups bound to the metal atom are quadruplet with δ equal to 0.57 ppm, and those of methyl groups give a triplet signal with δ of 1.26 ppm. Meanwhile, the signals of the above groups in the complex of triethylgallium and diethyl ether have δ equal to 0.99 and 1.53 ppm respectively. This product is technical.

The purity of the compound (Table 1), as regards the content of trace impurities, does not comply with the MOVPE requirements, because the product is contaminated with impurities of various elements and contains a fair amount of ether. The product can contain two types of impurities: 1) volatile impurities, and 2) non-volatile fine fractions slightly soluble in the product. The second type of impurities can be easily eliminated by distillation. Volatile impurities are usually ethyl derivatives of metals. The impurities under consideration can be inducted in the technical product by two ways: 1) metal Ga contains the residual elements which can be chlorinated and give trace impurities. The subsequent alkylation of

Table 2Dependence of GaEt₃ yield on mole ratio EtMgBr/GaCl₃.

Mole ratio EtMgBr/GaCl ₃	4.4	4.0	3.6	3.5	3.4	3.3	3.2
GaEt ₃ yield, %	98	97	98	96	98	87	75

GaCl₃ results into the alkylation of the resultant impurity chlorides; 2) metal Mg used in preparation of EtMgBr contains various impurities either in the form of elements or in the form of compounds with Mg. While GaCl₃ is alkylated with the Grignard reagent, the impurity elements contained in the initial magnesium can be reduced and/or alkylated. Thus, the chlorination of metal Ga followed by its alkylation results in the formation of a number of impurities in the form of ethyl derivatives of various elements. Depending on their physical and chemical properties, they might lead to difficulties in the purification of the end product. The main source of impurities is the Grignard reagent (Table 1). We have established that the most difficult process is to eliminate volatile silicon and zinc impurities that exist in the form of completely ethylated compounds with relatively close to GaEt₃ boiling temperatures 153–154 and 117 °C respectively. In this paper the various purification techniques which have allowed to obtain the product with such a level of trace impurities as required for MOVPE processes have been studied in detail.

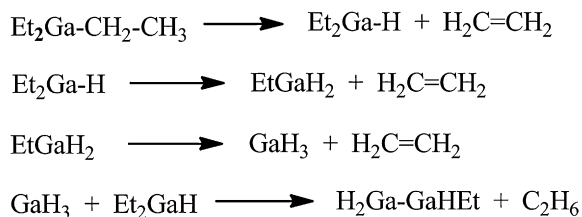
Good results on the removal of the residual ether have been obtained using double rectification of technical GaEt₃ at atmospheric pressure. Boiling temperature of the product under these conditions is about 143 °C, which is higher than dissociation temperature of Et₂O:GaEt₃ complex, and makes it possible to isolate the end product with ether content of about 40 ppm that does not exceed the value permissible for a majority of MOVPE applications. Vacuum rectification of Et₂O and GaEt₃ characterized by strong intermolecular interaction is impossible because a key separation factor is thermal dissociation of Et₂O:GaEt₃ complex that cannot be performed under such conditions. In other words, a decrease of the process temperature causes less effective operation of the rectification column.

The atmospheric rectification is generally labor-consuming, because it requires the second rectification of numerous initial and intermediate fractions. Moreover, an essential disadvantage of this technique is a loss of the expensive product resulted from a gradual accumulation of ethyldigalliumhydride in the still of the rectification column. It forms at temperatures above 160 °C as a result of the decomposition of GaEt₃. It has been detected using chromatography-mass spectrometry of the rectification residue from the peak with *m/z* of 174–172–170 [M⁺⁺] that indicates a molecular ion of ethyldigalliumhydride with its subsequent fragmentation into characteristic ions with *m/z* of 146–144–142 [M–C₂H₄]⁺, 73–71 [GaH₂]⁺ and 28 [C₂H₄]⁺. The formation route of the bimetal derivative is confirmed by ethane and ethylene found in the gas

Table 1Trace impurities in metal Ga; GaCl₃; and GaEt₃ obtained by various techniques based on ICP spectra.

Compound	Trace impurities, ×10 ⁻⁴ % w/w.														
	Al	Ba	Ca	Cd	Cr	Cu	Fe	Ge	Mg	Mn	Pb ^a	Si ^a	Sn ^a	Ti	Zn
Ga met. ^b	<0.2	<0.05	<0.05	<0.1	<0.2	<0.2	<0.1	<0.05	<0.05	<0.1	<0.1	<0.03	<0.05	<0.1	<0.1
GaEt ₃ techn	31.8	<0.05	<0.05	<0.2	<0.2	<0.3	1.5	<5.0	34.1	<0.1	5.0	2.5	5.0	<0.1	14.3
GaEt ₃ (purified using Al)	<0.5	<0.05	<0.05	<0.2	<0.2	<0.3	<0.3	<0.5	<0.05	<0.1	<3.0	<0.1	<0.3	<0.2	<0.3
GaEt ₃ (purified using GaCl ₃)	<0.5	<0.05	<0.05	<0.2	<0.2	<0.3	<0.3	<0.5	<0.05	<0.1	<3.0	<0.1	<0.3	<0.2	<0.3
GaEt ₃ (purified using rectification)	<0.5	<0.05	<0.05	<0.2	<0.2	<0.3	<0.3	<0.5	<0.05	<0.1	<3.0	<0.1	<0.3	<0.2	<0.3
GaEt ₃ (purified using complexation)	<0.5	<0.05	1.0	0.4	0.3	0.3	1.6	<0.5	0.06	<0.1	5.0	1.5	5.0	0.3	5.0
GaEt ₃ (vacuum rectification after purified using complexation)	<0.5	<0.05	<0.05	<0.2	<0.2	<0.3	<0.3	<0.5	<0.05	<0.1	<3.0	<0.1	<0.3	<0.2	<0.3

^a For volatile impurities of ethyl derivatives.^b The same results have been obtained for GaCl₃.



Scheme 2. Thermal decomposition of GaEt₃.

phase of the rectification products using ¹H NMR and mass spectroscopy and can be expressed by the following routes (Scheme 2).

The resultant gallium hydrides also react with diethyl ether to form ethoxydiethylgallium and triethoxygallium. Gallium ethoxides concentrate in the rectification residue. They can be detected using ¹H NMR spectroscopy by signals of O–CH₂ groups in the form of quadruplets with δ equal to 3.56 and 3.95 as well as using chromatography-mass spectrometry of the rectification residue from the peak with *m/z* of 174–172 that indicates a molecular ion [Et₂GaOEt]⁺ with its subsequent fragmentation into characteristic ions with *m/z* of 146–144 [M–C₂H₄]⁺, 118–116 [H₂GaOEt]⁺, 89–87 [H₂GaO]⁺, 87–85 [GaO]⁺, and the peak with 206–204 that indicates a molecular ion [Ga(OEt)₃]⁺ with its subsequent fragmentation into characteristic ions with *m/z* of 191–189 [M–CH₃]⁺, 161–159 [Ga(OEt)₂]⁺, 87–85 [GaO]⁺. Obviously, the formation of ethoxide derivatives results into the generation of ethanol which contributes to the reduction of the quantity of the purified triethylgallium by way of its alcoholysis. The resultant formation route for ethoxide derivatives can be expressed as follows (Scheme 3).

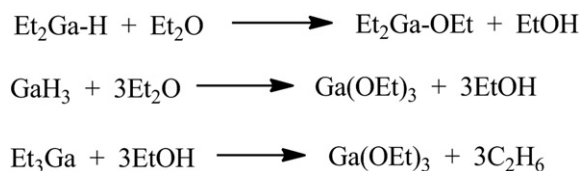
Since undesirable losses of the expensive end product are ca. 10%, we have tested alternative purification techniques for GaEt₃ including chemical bonding of both diethyl ether and triethylgallium, with the final vacuum rectification of triethylgallium.

It is known [14] that metal aluminum reacts with organogallium compounds by the following scheme (Scheme 4).

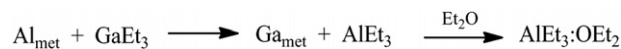
Unlike GaEt₃, the resultant AlEt₃ forms with the ether a more stable complex compound which is non-volatile during rectification. By adding into the still of the rectification column a 5 mol% excess of metal powder Al with respect to equimole quantity of the ether content, after the keeping of the reaction mixture at 100–120 °C for 2 h and a subsequent vacuum rectification of the end product at vapor temperature of 120 °C we have managed to obtain GaEt₃ with the ether content of ca. 30 ppm. Based on ICP results, the end product comply with the MOVPE requirements to the content of trace impurities (see Table 1).

An even lower content of the residual ether of 25 ppm in the end GaEt₃ is achieved by adding gallium trichloride into the still of the rectification column that forms diethylgalliumchloride with the alkyl derivative under the same conditions by the following scheme (Scheme 5).

Being a stronger Lewis acid than GaEt₃, diethylgalliumchloride, similarly to AlEt₃, forms with the ether a more stable and non-volatile complex compound which finally remains in the still of the rectification column. Based on NMR and mass spectra, no chlorine derivatives have been found in the end product.



Scheme 3. Generation of ethanol from Et₂O resulting from thermal decomposition of GaEt₃.



Scheme 4. Generation of AlEt₃ from GaEt₃ followed by its complexation with ether.

Among the disadvantages of the above chemical purification techniques reducing the content of the residual ether in triethylgallium a necessity of use of expensive high purity Al and GaCl₃ and a lower yield of the end product caused by its chemical reactions with the added reagents can be mentioned. Another great disadvantage of physical–chemical purification techniques using Al and GaCl₃ is the formation and accumulation of a big volume of pyrophoric rectification residue further unusable that greatly decreases device efficiency. A big amount of rectification residues is caused by a risk of ingress of uncomplexed reaction products, e.g. AlEt₃ into the end product. The data on trace impurities in GaEt₃ purified using those techniques are summarized in Table 1. Therefore we have studied a more attractive chemical purification technique by means of the complexation of triethylgallium also known as the adduct purification technique [3].

The technique is based on a different strength of the donor–acceptor interaction of various electron donors with Lewis acids. The donor–acceptor interaction strength is known to decrease for alkyl compounds of electron donors in the row of Groups 15 and 16 elements N > P > As > O > S > Se. Our speculation is based on the following assumptions: a) a stronger donor will displace the ether from its adduct with GaEt₃ to form a stronger complex compound; b) at the same time the newly formed complex will be thermally stable enough before it dissociates into its constituent molecules; c) the decomposition temperature of the complex should be lower than that of GaEt₃ (T_{thermal decomposition} > 160 °C; T_{boiling} = 143 °C). Moreover, boiling and decomposition temperatures of a new ligand should also be much higher than those of GaEt₃ to prevent this ligand or its decomposition products from getting into triethylgallium during and after the purification process.

Electron donors stronger than alkoxy groups contains Group 13 element (N, P, As) with a lone electron pair. Literature data analysis has shown that aliphatic [15–17], aromatic [18–21], fatty aromatic [19,20,22] and heterocyclic [12,23–26] amines of various structure form with organic gallium derivatives both intramolecular and intermolecular complexes. It has been shown as well that for diamines and tetramines the complexation goes stepwise, i.e. first with one nitrogen atom and then with the second, the third and the fourth heteroatoms. However, the donor–acceptor interaction strength of nitrogen compounds with GaR₃ described in literature is characterized by high values of formation enthalpy; therefore it is almost impracticable to destruct such complexes into constituent compounds under reasonable conditions. Any attempt of their thermal destruction leads as a rule to the formation of a covalent Ga–N bond and the elimination of unsaturated hydrocarbons [18,22,23]. Similar results have been obtained when we have attempted to purify triethylgallium by way of its complexation with N,N-dimethyldodecylamine. The initial GaEt₃ cannot be regenerated from the easily forming complex of Et₃Ga:N(Me)₂C₁₀H₂₁ by way of its heating up to 175 °C in vacuum of 1 Torr. Higher temperatures are inadmissible.

Our assumptions are confirmed by authors at Ref. [4], who went further in their attempt to study multidentate nitrogen donor ligands (4N- and 6N-aza crowns), which were used to purify the GaEt₃ (R = Et, Pr) compounds. They have developed a new



Scheme 5. Generation of Et₂GaCl from GaEt₃ followed by its complexation with ether.

advanced technique aimed at ultimate minimization of oxygen impurities. It should be also noted that the distilled complex with triethylamine contains aggregate metal impurities at the level of <1 ppm [4].

The complexation of alkylgallium compounds with phosphines has been described in references [11,12,24–26]. The most practicable interest is attracted by adducts of trimethyl derivatives of Al, Ga and In with triphenylphosphine and high-melting di-, tri- and tetraphos [11], such as $(\text{Me}_3\text{M})_2 \cdot (\text{Ph}_2\text{PCH}_2)_2$, $(\text{Me}_3\text{M})_3 \cdot (\text{Ph}_2\text{PCH}_2\text{CH}_2)_2\text{PPh}$ and $(\text{Me}_3\text{M})_4 \cdot (\text{Ph}_2\text{PCH}_2\text{PPhCH}_2)_2$. The authors have shown that the complexation of the above mono- and polyphosphines leads to a formation of ether-free adducts that are able to regenerate metal trialkyls during the heating in vacuum of 0.01 Torr with the yield of 45–93%. Eventually it has been concluded that a low vapor pressure of phosphines and the presence of electron-acceptor phenyl substituents in them is determinative for a successful formation of relatively weak adducts that are able to displace the ether and regenerate into constituent components.

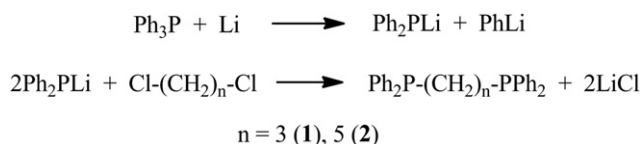
Based on general considerations and available facts, the following requirements to phosphorus-containing ligands suitable for the adduct purification of trialkyl compounds of Al, Ga and In can be formulated: a) easy formation of $\text{L}^{\text{P}}:\text{MAlk}_3$ adducts; b) a complete displacement of the ether from $\text{Et}_2\text{O}:\text{MAlk}_3$; c) a possibility to carry out a preparative synthesis of a ligand and its scaling; d) a possibility to regenerate a ligand and a metal trialkyl; e) a ligand stability in the operating temperature range; f) a low volatility during the decomposition of adducts with metal trialkyls.

In view of the above and a well-known fact that a melting temperature of tetraphenyldiphosphinealkanes of $\text{Ph}_2\text{P}-(\text{CH}_2)_n-\text{PPh}_2$ type with end phosphine groupings tends to decrease in case of odd values n (melting temperature for $n = 2-6$ is 144, 62, 133, 42 and 127 °C respectively [27]), it has seemed reasonable to study a possibility of reversible complexation not only for methyl but also for ethyl compounds of Ga which are in greater demand in MOVPE as well as of other Group 13 metals such as Al and In with triphenylphosphine and low-melting, low-volatile bis(diphenylphosphine)alkanes (**1** and **2**).

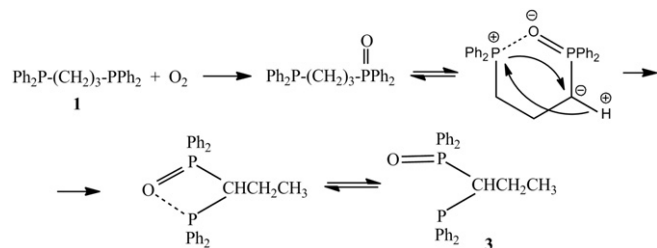
The original diphosphines have been synthesized by a reaction of respective dichlorides with diphenylphosphenelithium by the basic methodology described in Ref. [28] by the following scheme (Scheme 6).

When the resultant phenyllithium is deactivated as described in the methodology [29] by adding an equimole quantity of tert-butylchloride followed by the processing of the reaction mixture with alkanedichlorides, the yield of compounds **1** and **2** is 17 and 21% respectively. When phenyllithium is not deactivated and a mixture of lithium derivatives is directly alkylated by excess alkanedichlorides, reaction products are partitioned through their fractional precipitation with aqueous methanol with subsequent recrystallization, the yield of alkanediphosphines **1** and **2** has increased up to 35% of the theoretical one. In order to ensure success, it is highly important to carry out the reaction in the dry argon. Otherwise, as established for 1,3-dichlorinepropane, the yield falls owing to an oxidative isomerization of the diphosphine accompanied by a 1,3-sigmatropic shift of the diphenylphosphine grouping by the following scheme (Scheme 7).

The rearrangement probably occurs through a six-membered cyclic transition state and is conditioned by the interaction of



Scheme 6. Synthesis of bis(diphenylphosphine)alkanes.



Scheme 7. Oxidation of 1,3-bis(diphenylphosphine)propane.

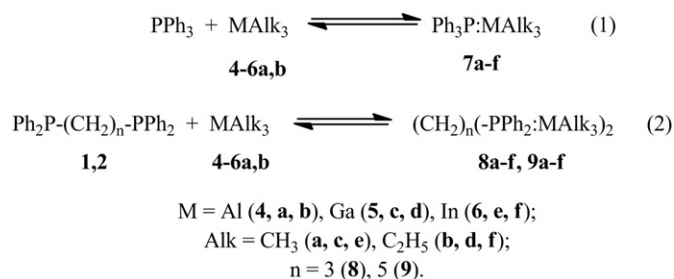
phosphorus and oxygen atoms which makes possible a protonotropy and ionotropy of the diphenylphosphine grouping.

The structure of compound **3** has been determined on the basis of mass spectra characterized by the peak of the molecular ion with m/z 428; ^1H NMR spectra containing a characteristic signal of protons of the CH-group in the form of quadruplet at δ 3.58 ppm, a signal of protons of the CH_2 -group in the form of multiplet at δ 1.65 ppm and a characteristic signal of protons of the CH_3 -group in the form of triplet at δ 1.26 ppm; IR spectra showing absorption bands of P–O–P vibrations with frequency of 948 cm^{-1} and P=O vibrations with ν 1183 cm^{-1} ; as well as elemental analysis results. No characteristic splitting of signals of the CH_2 -group at the chiral center on the ^1H NMR spectra and the appearance of the band of P–O–P vibrations on the IR spectra evidence a hindered rotation around the C–P bond that is obviously conditioned by the interaction of the oxygen atom with the both phosphorus atoms.

The formation of compound **3** not only reduces a yield of the end diphosphine **1**, but also greatly impedes its isolation by means of recrystallization.

Adducts of trimethyl and triethyl derivatives of Al, Ga and In have been synthesized by dripping benzene solutions of phosphines. In all cases the formation of complexes **7a–f**, **8a–f** and **9a–f** is accompanied by weak exothermic effect by the following scheme (Scheme 8).

The resultant complexes **7a–f**, **8a–f** and **9c** are white crystalline substances, which readily crystallize from concentrated benzene solutions; complexes **9a,b,d–f** have been isolated in the form of thick oils. Their structure has been confirmed by the elemental analysis and the NMR spectra given in Table 3. A comparison of spectra of original metal trialkyls, phosphines and diphosphines with those of their adducts explicitly evidences a complexation between them. It appears on ^1H NMR spectra as downfield resonance shifts of alkyl substituents bound to metal atoms, with the shift being the highest in case of aluminum for methyl derivatives. The complexation is also detected by downfield resonance shifts of protons of the methyl group, which is distant from the metal atom. Meanwhile, resonances of the CH_2 -group bound to the phosphorus atom demonstrate the upfield shift in an alkyl part of the diphosphine ligand of bis(diphenylphosphine)propane complexes **8a–f** that is also indicative for decreasing of acceptor properties of



Scheme 8. Reversible complexation of MAlk_3 ($\text{M} = \text{Al, Ga, In}$; $\text{Alk} = \text{Me, Et}$) with organophosphine ligands.

Table 3
 ^1H and ^{31}P NMR shifts of initial compounds and their complexes in C_6D_6 .

No.	Compound	δ_{H} , ppm			δ_{P} , ppm
		MR ₃	Phosphine		
			Alkyl	Aryl	
–	Ph_3P	–	–	7.44 (m, 6H); 7.01 (m, 9H)	–6.26
1	$\text{Ph}_2\text{P}-(\text{CH}_2)_3-\text{PPh}_2$	–	2.12 (m, 4H); 1.72 (m, 2H)	7.44 (m, 6H); 7.01 (m, 9H)	–17.68
2	$\text{Ph}_2\text{P}-(\text{CH}_2)_5-\text{PPh}_2$	–	1.98 (m, 4H); 1.51 (m, 4H); 1.45 (m, 2H)	7.43 (m, 8H); 7.10 (m, 12H)	–16.35
4a	AlMe_3	–0.35 (s, 9H)	–	–	–
4b	AlEt_3	1.16 (t, 9H); 0.35 (q, 6H)	–	–	–
5a	GaMe_3	–0.10 (s, 9H)	–	–	–
5b	GaEt_3	1.26 (t, 9H); 0.57 (q, 6H)	–	–	–
6a	InMe_3	–0.18 (s, 9H)	–	–	–
6b	InEt_3	1.48 (t, 9H); 0.6 (q, 6H)	–	–	–
7a	$\text{Ph}_3\text{P} \cdot \text{AlMe}_3$	–0.07 (s, 9H)	–	7.52 (m, 8H); 7.17 (m, 12H)	–5.21
7b	$\text{Ph}_3\text{P} \cdot \text{AlEt}_3$	1.52 (t, 9H); 0.60 (q, 6H)	–	7.49 (m, 6H); 7.08 (m, 9H)	–5.25
7c	$\text{Ph}_3\text{P} \cdot \text{GaMe}_3$	0.29 (s, 9H)	–	7.50 (m, 6H); 7.05 (m, 9H)	–5.25
7d	$\text{Ph}_3\text{P} \cdot \text{GaEt}_3$	1.55 (t, 9H); 0.96 (q, 6H)	–	7.49 (m, 6H); 7.04 (m, 9H)	–4.35
7e	$\text{Ph}_3\text{P} \cdot \text{InMe}_3$	0.24 (s, 9H)	–	7.52 (m, 6H); 7.05 (m, 9H)	–6.72
7f	$\text{Ph}_3\text{P} \cdot \text{InEt}_3$	1.71 (t, 9H); 1.06 (q, 6H)	–	7.48 (m, 6H); 7.10 (m, 9H)	–6.13
8a	$(\text{CH}_2)_3(\text{PPh}_2 \cdot \text{AlMe}_3)_2$	–0.05 (s, 9H)	2.10 (q, 4H); 1.54 (m, 2H)	7.52 (m, 6H); 7.12 (m, 9H)	–18.56
8b	$(\text{CH}_2)_3(\text{PPh}_2 \cdot \text{AlEt}_3)_2$	1.32 (t, 9H); 0.32 (q, 6H)	1.97 (q, 4H); 1.57 (m, 2H)	7.42 (m, 8H); 7.07 (m, 12H)	–15.29
8c	$(\text{CH}_2)_3(\text{PPh}_2 \cdot \text{GaMe}_3)_2$	0.08 (s, 9H)	2.01 (q, 4H); 1.70 (m, 2H)	7.35 (m, 8H); 7.05 (m, 12H)	–12.58
8d	$(\text{CH}_2)_3(\text{PPh}_2 \cdot \text{GaEt}_3)_2$	1.35 (t, 9H); 0.68 (q, 6H)	2.03 (q, 4H); 1.60 (m, 2H)	7.42 (m, 8H); 7.11 (m, 12H)	–12.34
8e	$(\text{CH}_2)_3(\text{PPh}_2 \cdot \text{InMe}_3)_2$	0.10 (s, 9H)	2.07 (q, 4H); 1.71 (m, 2H)	7.37 (m, 8H); 7.08 (m, 12H)	–17.68
8f	$(\text{CH}_2)_3(\text{PPh}_2 \cdot \text{InEt}_3)_2$	1.60 (t, 9H); 0.85 (q, 6H)	2.08 (q, 4H); 1.71 (m, 2H)	7.43 (m, 8H); 7.11 (m, 12H)	–15.86
9a	$(\text{CH}_2)_5(\text{PPh}_2 \cdot \text{AlMe}_3)_2$	–0.1 (s, 9H)	1.95 (q, 4H); 1.45 (m, 4H); 1.25 (m, 2H)	7.44 (m, 8H); 7.14 (m, 12H)	–15.82
9b	$(\text{CH}_2)_5(\text{PPh}_2 \cdot \text{AlEt}_3)_2$	1.23 (t, 9H); 0.38 (q, 6H)	2.03 (q, 4H); 1.42 (m, 4H); 1.25 (m, 2H)	7.45 (m, 8H); 7.10 (m, 12H)	–14.40
9c	$(\text{CH}_2)_5(\text{PPh}_2 \cdot \text{GaMe}_3)_2$	0.2 (s, 9H)	1.97 (q, 4H); 1.43 (m, 4H); 1.23 (m, 2H)	7.47 (m, 8H); 7.10 (m, 12H)	–14.26
9d	$(\text{CH}_2)_5(\text{PPh}_2 \cdot \text{GaEt}_3)_2$	1.54 (t, 9H); 0.87 (q, 6H)	2.00 (q, 4H); 1.43 (m, 4H); 1.23 (m, 2H)	7.44 (m, 8H); 7.05 (m, 12H)	–13.14
9f	$(\text{CH}_2)_5(\text{PPh}_2 \cdot \text{InEt}_3)_2$	1.67 (t, 9H); 0.98 (q, 6H)	2.03 (q, 4H); 1.47 (m, 4H); 1.28 (m, 2H)	7.43 (m, 8H); 7.10 (m, 12H)	–14.75

diphenylphosphine substituents as a result of complexation. This effect is decreased, when an alkyl chain is extended in compounds **9a–f**. Phosphorus resonance shifts for most adducts downfield on ^{31}P NMR spectra due to complexation.

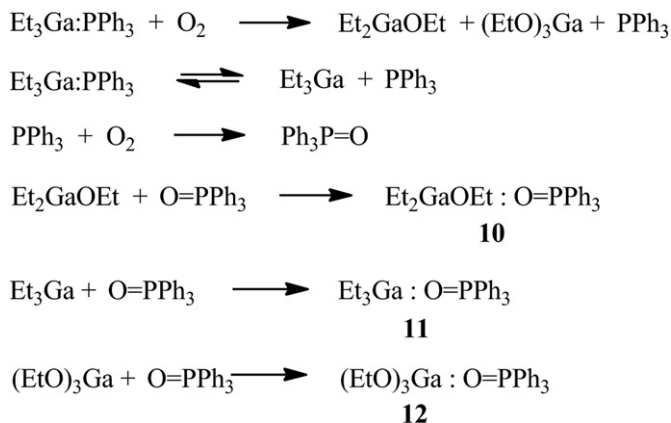
It should be noted that downfield shifts $\Delta\delta_{\text{H}}$ for alkyl substituents bound to the metal atom for the studied complexes **7–9** which are determined as the difference of δ_{H} values of a coordinate and a free metal trialkyl, change in the following order $\text{PPh}_3 \geq \mathbf{2} \geq \mathbf{1}$ depending on the phosphine nature. An ability of the phosphorus atom defined by the nature of its substituents to form complexes should theoretically change in the following order $\mathbf{2} \geq \mathbf{1} > \text{PPh}_3$. Hence, the value of chemical shifts δ_{H} in complexes **7–9** does not correlate with the strength of the M–P bond which is apparently caused by the donor properties of the phosphine groups different in direction and the steric repulsion of alkyl groups bound to the metal atom and the substituents bound to the phosphorus atom [30]. The same conclusion can be made from the absence of the correlation between phosphorus chemical shifts $\Delta\delta_{\text{P}}$ for the studied complexes **7–9** and the nature of metal trialkyl. The values of $\Delta\delta_{\text{P}}$ are determined as a difference of δ_{P} values of a coordinate and a free phosphine, with the nature of metal trialkyl. In this case values of $\Delta\delta_{\text{P}}$ can correlate only with a steric branching of phosphine. This has been previously shown by the example of complexes of AlMe_3 with various phosphines [31].

It should be noted that in diluted solutions of complexes **7–9** in benzene and chloroform the above compounds have not dissociated during both long stay at room temperature and long heating to 60 °C. A slow dissociation of the complexes occurs only at temperatures above 65 °C.

Complexes **7–9** are far more resistant to atmospheric oxygen as compared with the original metal trialkyls. No spontaneous inflammation in the air has been observed; the white smoke indicative of an active stage of oxidation for most complexes has appeared after staying in the air for 5–10 min. The oxidative stability of the synthesized adducts **7–9** has been studied on a 5% solution of the complex of triethylgallium with triphenylphosphine

(**7d**) in benzene under atmospheric oxygen using NMR spectrometry in a sealed vial with a liquid–gas interface. It has been established that the oxidation starts with the formation of ethoxydiethylgallium and small quantities of triethoxygallium. Their generation is detected by ^1H NMR studies from the signals of O–CH₂ fragments as quadruplets with δ 3.56 and 3.95 ppm. However, as one ethyl group of GaEt_3 has converted by 10% into an ethoxy group, a gradual dissociation of complex **7d** into GaEt_3 and PPh_3 has been observed and shown in the spectra as resonances of free GaEt_3 with δ 0.63 and 1.33 ppm. The isolated PPh_3 is oxidized by atmospheric oxygen into triphenylphosphineoxide that is clearly seen in the spectra by the appearance and the intensification of the resonance of protons in the position 2 and 6 of the phenyl substituents of the Ph_3PO molecule as quadruplet with δ 7.78 ppm. Besides, as a result of autocatalytic oxidation processes of the phosphine moiety of complex **7d**, the speed of the Ph_3PO formation becomes higher than the speed of the Ga–C oxidation that leads to an increase of the triphenylphosphineoxide concentration. The oxidation process finally results in a mixture of complexes of triphenylphosphineoxide with ethoxydiethylgallium (**10**), triethylgallium (**11**) and triethoxygallium (**12**) in mole ratio 1:1:0.2 (Scheme 9).

Dative bond O:→Ga is obviously less stable than P:→Ga that leads to a lower downfield shift during the complexation with triphenylphosphineoxide. Therefore the resultant ^1H NMR spectra of the mixture that forms after the oxidation of complex **7d** contain characteristic resonances of protons of complex **10** in the form of triplets at δ 1.56 (CH₃ from the ethyl group) and 1.16 ppm (CH₃ from the ethoxy group) and quadruplets of CH₂ and OCH₂-groups at δ 0.8 and 3.2 ppm. As regards the complex **11**, the signals of CH₂-groups are observed as triplet at δ 1.44 ppm and quadruplet at δ 0.75 ppm. Triethoxygallium complex **12** is represented in the ^1H NMR spectra by signals of ethoxy groups in the form of quadruplet at δ 3.62 ppm and triplet at δ 1.16 ppm. Resonances of aromatic substituents are registered in the form of multiplet at δ 7.15 ppm and quadruplet at δ 7.81 ppm. Meanwhile, mass spectra of a mixture



Scheme 9. Oxidation of $\text{Et}_3\text{Ga}:\text{Ph}_3\text{P}$ and formation of by-products.

of complexes **10–12** contain peaks of molecular ions $[\text{Et}_2\text{GaOEt}]^+$ (m/z 174–172), $[(\text{EtO})_3\text{Ga}]^+$ (m/z 206–204), $[\text{GaEt}_3]^+$ (m/z 158–156) and $[\text{Ph}_3\text{PO}]^+$ (m/z 278) that indicates a decomposition of the complexes into components during the electron impact.

A similar flow of oxidation through time has been observed in ^1H NMR spectra for 3–5% solutions of complexes **7b,c** and **8b,d** in chloroform and benzene.

Since the synthesized complexes **7–8** and complex **9c** easily crystallize from saturated benzene solutions, we have managed to obtain single crystals of appropriate quality and study their structure using X-ray diffraction. These studies have been of obvious practical interest, because the geometry of phosphine complexes is known to have a great influence on the rate of their dissociation reaction [30]. Figs. 1–13 show molecular structures of complexes **7–9**; values of bond lengths and bond angles are given in Tables 4–8. It has also been established that bis(diphenylphosphine)propane complexes **8a–f** analyzed by X-ray diffraction and containing a fragment of MMe_3 as well as InEt_3 are isostructural and crystallize in a monoclinic cell. A relative arrangement of both MAlk_3 fragments in the crystals can be described as *anti*-clinalic (a corresponding pseudo-torsion angle is $95.5 \div 97.5^\circ$). Molecules **8a–9c** (except of compound **8d**) crystallize with solvate benzene molecules located in the channels in crystal packing between molecules of the complexes. All intermolecular

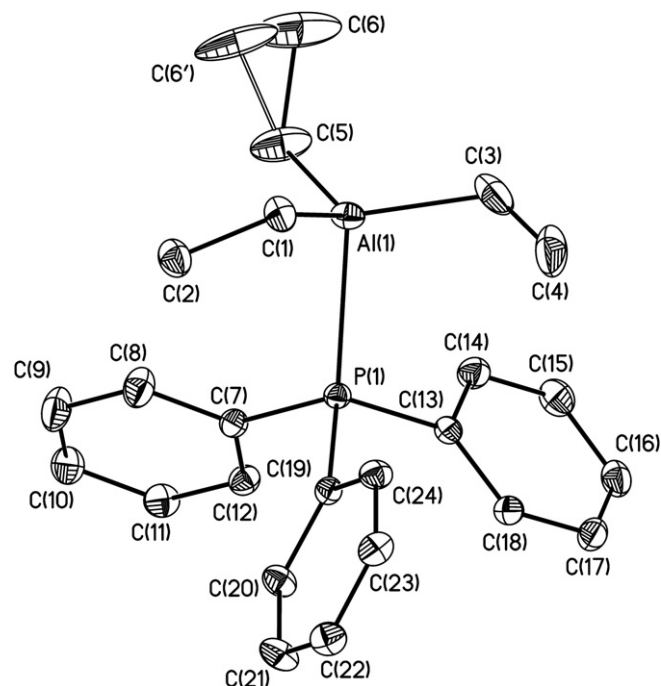


Fig. 2. Molecular structure of compound **7b**.

contacts with C_6H_6 molecules correspond to weak intermolecular interactions $\text{H}\cdots\text{H}$.

To characterize the strength of metal–phosphorus donor–acceptor bonds in more detail, complexes of metal trialkyls with triphenylphosphines have been studied as comparison compounds. First of all, it should be noted that M–P bonds in complexes **7a–9c** are 0.01–0.04 Å shorter than those in complexes of MMe_3 with bis(diphenylphosphine)ethane [11]. A possible reason is the differences in donor ability of the bis(diphenylphosphine)ethane as compared to the bis(diphenylphosphine)propane. Also, the structural data on the complexes in Ref. [11] were collected at room temperature, so the thermal motion can be another reason that can partially explain

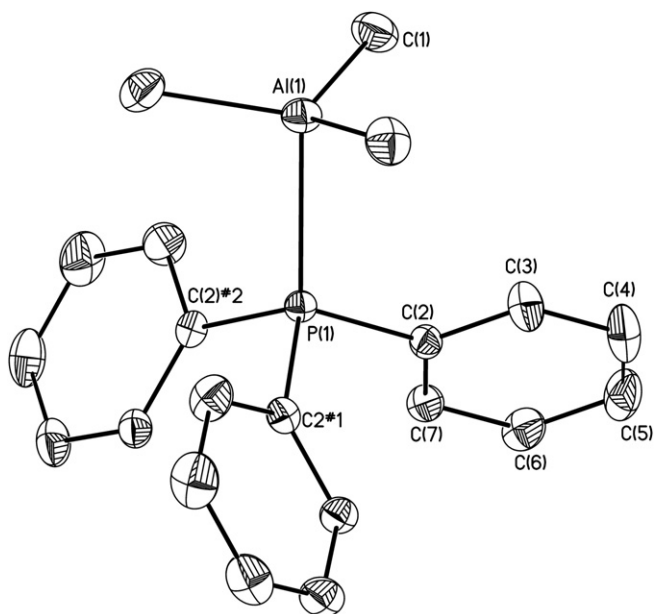


Fig. 1. Molecular structure of compound **7a**.

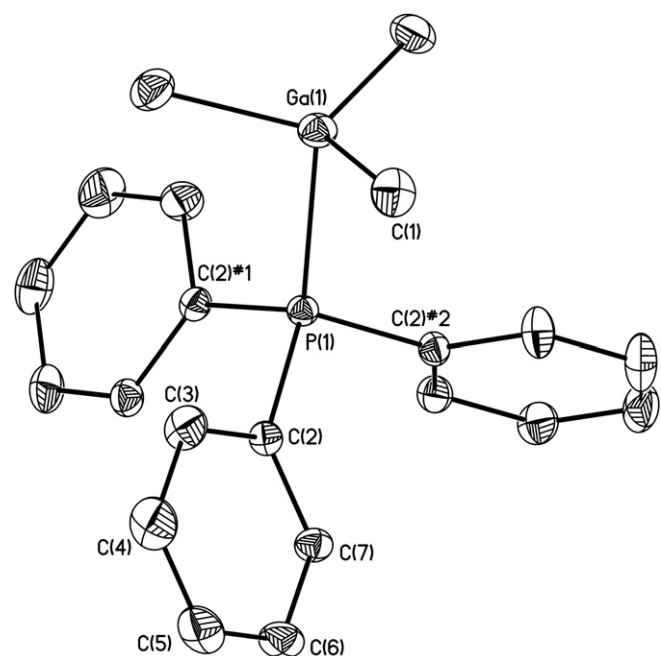


Fig. 3. Molecular structure of compound **7c**.

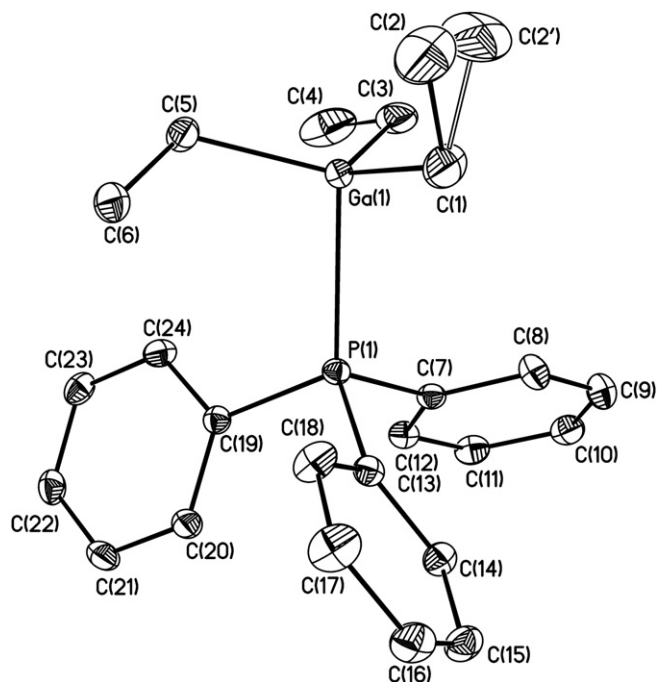


Fig. 4. Molecular structure of compound 7d.

the above-mentioned differences. In complexes **7a–f** lengths of M–P donor–acceptor bonds vary in the range of 2.53–2.73 Å, with maximum values observed for M = In and Alk = Et. It should be noted that interatomic distances M–P for alkylgallium complexes are only 0.03–0.04 Å greater than those for alkylaluminum complexes. If Al or Ga is replaced by In, the length of M–P bonds and M–C bonds increases by 0.2 Å that conforms to differences in ion radii of these elements [32]. In complexes with Alk = Et (**7b**, **7d**, **7f**) the lengths of M–P bonds slightly (by 0.01 Å) exceed those in complexes **7a**, **7c**, **7e** (Alk = Me). Generally these tendencies hold true for complexes **8a–f** too, but M–P bonds appear to be 0.03 Å shorter than those in complexes with PPh₃. Probably, the replacement of an acceptor phenyl substituent in triphenylphosphine by an alkyl chain results in

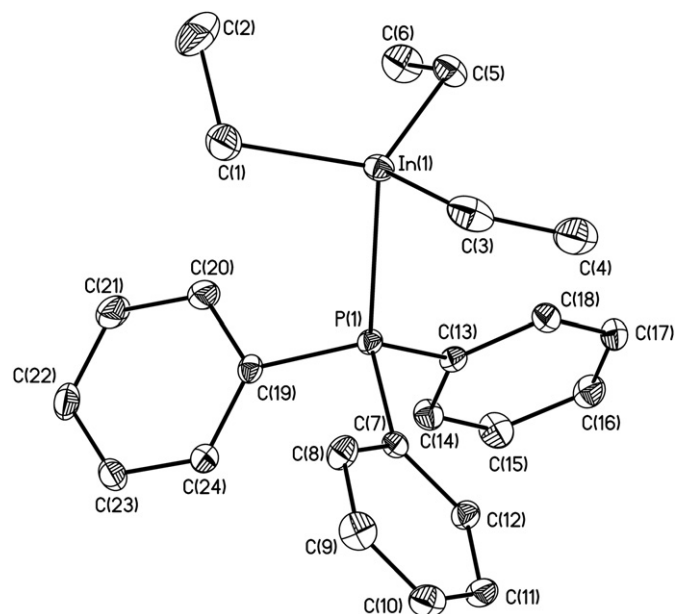


Fig. 6. Molecular structure of compound 7f.

increased donor ability of P atom and somewhat more stable M–P bond. The replacement of Me radicals by Et ones in metal atom coordination environments decreases an acceptor ability of those metals. At the same time, when substituents bound to the Al atom vary, differences in M–P bond lengths are 0.02 Å, while they are much greater in similar Ga and In complexes and reach 0.05 Å (Tables 7 and 8). The M–C bond in the case of Et substituents is only slightly (*ca* 0.01 Å) longer than that in the case of Me ones. Anyway, the M–C in the complexes investigated in present paper is 0.03–0.04 Å shorter than that in the complexes of 1,4-diazabicyclo[2.2.2]octane with AlMe₃ and GaMe₃. It allows us to conclude that the greater is an atomic number, the higher are steric hindrances in the metal coordination environment. This factor probably causes a greater than expected downfield shift $\Delta\delta_H$ of resonances of alkyl substituents bound to a metal atom in indium complexes as compared to that in Ga complexes. The downfield shift $\Delta\delta_H$ is given in Table 9.

Thus, based on the X-ray diffraction analysis data it can be expected that the easiness of thermal dissociation of synthesized complexes **7–9** decreases in a metal row In > Ga ≥ Al, in a row of phosphines PPh₃ > **1** ≥ **2** and in a row of alkyl substituents bound to

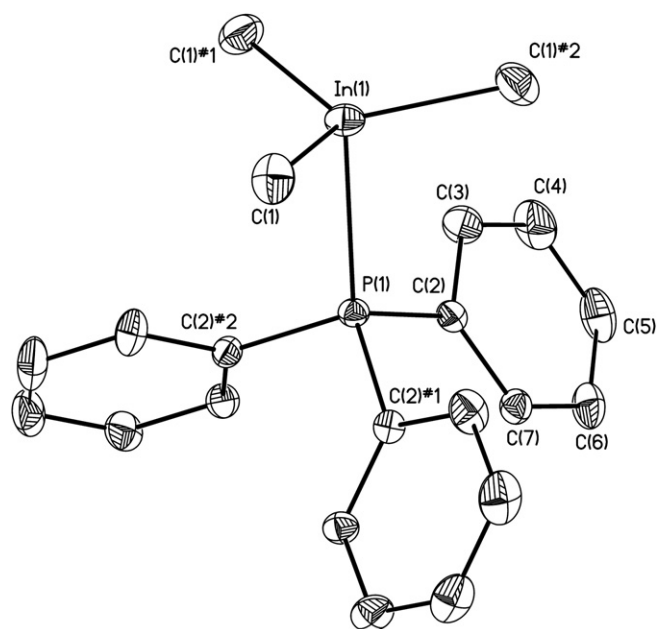


Fig. 5. Molecular structure of compound 7e.

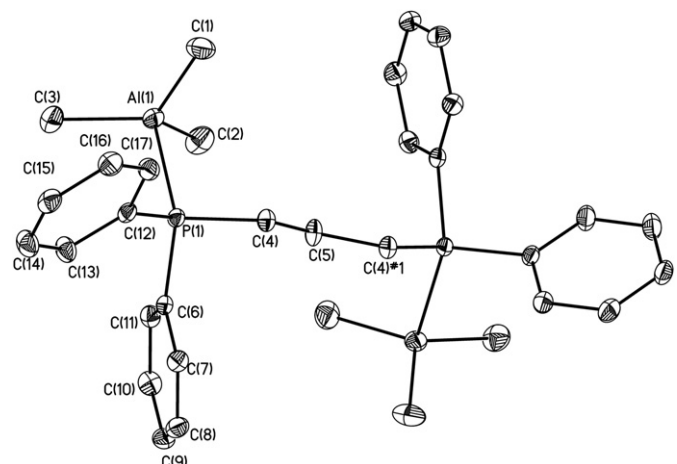
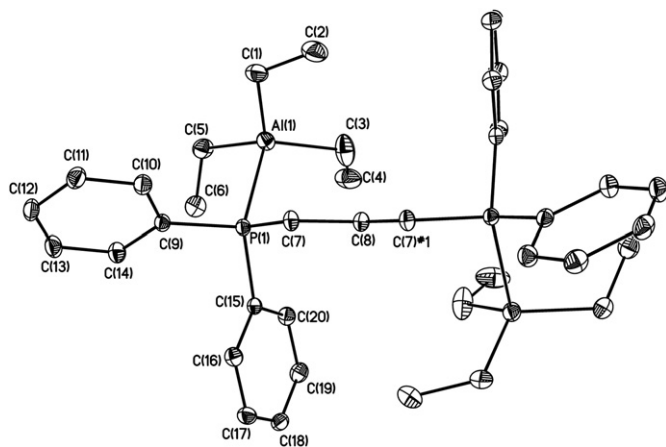


Fig. 7. Molecular structure of compound 8a.

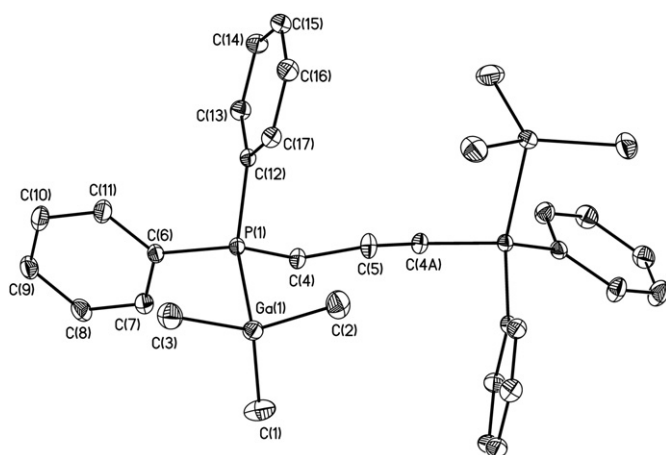
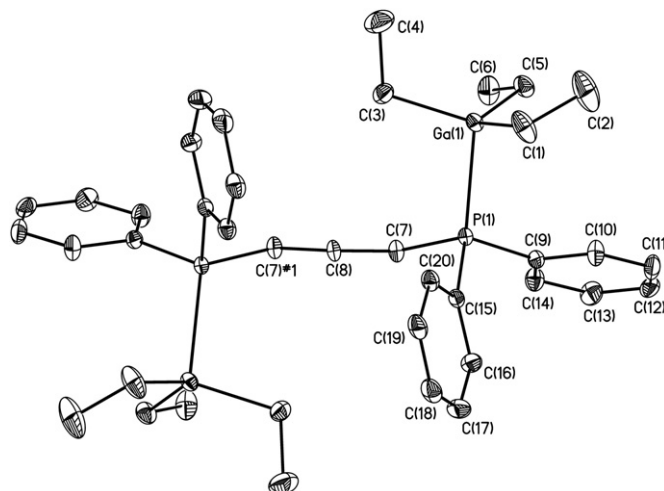
Fig. 8. Molecular structure of compound **8b**.

a metal atom $\text{Et} > \text{Me}$. However, since a dissociation constant of adducts in case of diphosphines is proportional to a square partial pressure of metal trialkyls over their adducts [11], the dependence of the easiness of thermal dissociation of complexes **7–9** on the phosphine nature is not obvious and requires an experimental check.

Quantum chemical calculations (PBE0/6-311G(d,p)) have been made to analyze in more detail the dependence of a nature of a phosphine complex and its tendency to dissociation. Structural parameters of isolated molecules, values of dissociation energies (D_e) of M–P bonds as well as values ΔH_{398} and ΔG_{398} of dissociation have been identified (Table 10). In the isolated molecules M–P bonds are 0.03–0.07 Å longer than those in a crystal that is characteristic of donor–acceptor complexes during their transition from a condensed state to the gas phase [33].

The analysis of D_e values has shown that the strength of complexes decreases from Al to In and when MMe_3 is replaced by MEt_3 . This conforms to the distribution of M–P bond lengths. M–P bonds in complexes **8a–f** are only a bit stronger than those in complexes **7a–f**. On the other hand, complexes **8** are more thermodynamically stable at 398 K. No definite correlation between M–P bond lengths and values of thermodynamic parameters ΔH_{398} and ΔG_{398} is observed.

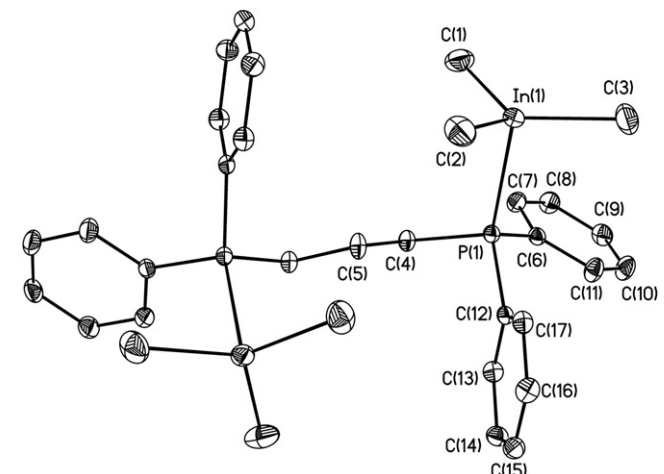
A thermogravimetric analysis of synthesized gallium complexes **7d** and **8c,d** confirms the data of the above researches. A thermogram of the above compounds clearly displays temperature peaks without any mass variation or with a slight mass loss of the samples

Fig. 9. Molecular structure of compound **8c**.Fig. 10. Molecular structure of compound **8d**.

that indicate transitions to a liquid state and the removal of crystallization benzene. Visible mass losses are observed at temperatures of ca. 100, 125 and 145 °C respectively. Trialkylgallium splits out at up to 305–310 °C. In case of higher temperatures a slope ratio of a line tangent to a mass curve increases sharply that is caused by the commencement of phosphine evaporation processes. Meanwhile, a total yield of the trialkylgallium from adducts **7d** and **8c,d** is 75, 91 and 99% respectively, and the thermogram shows peaks of various intensity, primarily endothermic ones, that clearly indicate triethyl- and trimethylgallium decomposition processes.

Thus, adduct purification of compounds **4–6** at atmospheric pressure does not seem feasible. A way out is to perform a decomposition process in vacuum. As we have ascertained by example of complexes **7d** and **8d**, their reversible dissociation into an original phosphine or diphosphine and triethylgallium in vacuum of 1 Torr becomes visible at temperatures above 80 °C (Scheme 10).

A high volatility of triethylgallium allows us to remove it from the melt of complexes **7d** and **8d** in vacuum and uninterruptedly shift the equilibrium to the formation of original components. Thus, triethylgallium purification has been performed in three stages. At the first stage GaEt_3 containing 4–5% diethyl ether interacts with 5 mol% Ph_3P or 0.55 mol 1,3-bis-(diphenylphosphine)propane to form adducts **7d** and **8d**. Vacuumization of the resultant complexes at 70 °C has allowed us to completely remove diethyl ether. At the third stage the complexes have been heated in vacuum to regenerate

Fig. 11. Molecular structure of compound **8e**.

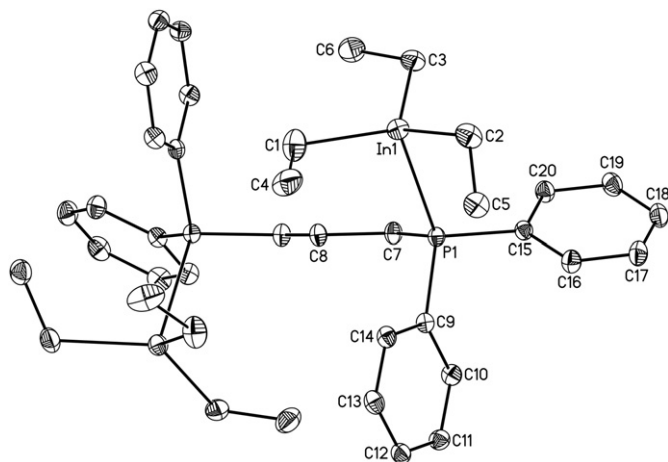


Fig. 12. Molecular structure of compound 8f.

triethylgallium, which is distilled in vacuum, and an appropriate phosphine, which can be reused for subsequent operations of deep purification. The yield of high purity GaEt₃ by way of formation of adducts **7d** and **8d** has been 93 and 95% respectively, with the parameters of the third stage of the process limited to 120–125 °C, vacuum of 1 Torr and 2–3 h.

A similar purification procedure for compounds **4–6** has been tested using reversible complexation of adducts **7–9** according to equations (1) and (2) (Scheme 8). Data on the yield of alkyl derivatives of Group 13A metals are given in Table 11.

The adduct technique makes it possible to purify metal trialkyls from such usual oxygen impurities as dialkyl metal alkoxides which can form at the stage of synthesis. As a rule, their content in a technical product is negligible. They form stronger coordination compounds with ligands than metal trialkyls do and remain in the still, while a metal trialkyl is segregating. At the stage of segregation it is particularly important to maintain a temperature which rules out a dissociation of complexes of alkoxides with ligands. Gradually accumulating in the still (ligand), alkoxide impurities can deteriorate quality of adduct purification; besides, a probability that alkoxides will get into the end product grows. After a few purification processes the ligand is regenerated.

It should be noted that a lower yield of ethyl derivatives of aluminum and indium is probably conditioned by their boiling temperatures. In order to increase a yield of the regenerated AlEt₃ and InEt₃, it is obviously required to use a deeper vacuum that is acceptable for their isolation from phosphines, but not sufficient for

Table 4
Bond lengths (Å) and angles (°) for Ph₃P:MMe₃ (**7a,c,e**).

Bond length/Å or angle (°)	Compound		
	7a M = Al	7c M = Ga	7e M = In
M(1)–C(1)	1.9781(10)	1.9908(9)	2.1800(8)
M(1)–P(1)	2.5329(6)	2.5375(5)	2.7333(2)
P(1)–C(2)	1.8174(8)	1.8177(7)	1.8167(5)
C(1)–M(1)–C(1')	116.63(2)	116.929(15)	118.169(12)
C(1)–M(1)–P(1)	100.70(3)	100.21(3)	97.84(3)

Symmetry code(s): (i) –y, x – y, z.

evaporation of the latter. From this perspective, a use of high-boiling compound **2** seems more preferred.

3. Conclusion

Thus, we have ascertained that one of the most optimal fabrication technique for high purity GaEt₃ suitable for application in epitaxial growth of semiconductor layers using MOVPE is direct chlorination of metal Ga, followed by processing of the resultant gallium trichloride with EtMgBr in diethyl ether at mole ratio 1/3.4. Deep purification of GaEt₃ from the ether can be performed using both multiple rectification and interaction with high purity Al and GaCl₃ as well as by way of reversible complexation with Ph₃P or Ph₂P–(CH₂)_n–PPh₂ (n = 3, 5). During rectification at atmospheric pressure the product partially decomposes to form EtGa₂H₃, Et₂GaOEt and (EtO)₃Ga. The most effective techniques of deep purification include physical–chemical purification using Al and GaCl₃ followed by vacuum rectification and reversible complexation with phosphines also suitable for other Ga, Al and In trialkyls with final rectification of the end product in vacuum at vapor temperature 120 °C which is far lower than decomposition temperature of GaEt₃. X-ray diffraction analysis of the structure of phosphine complexes has shown that a replacement of an acceptor phenyl substituent in triphenylphosphine by an alkyl chain results into higher donor ability of P atom and a stronger metal–phosphorus bond. In its turn, the replacement of Me radicals by Et radicals in the coordination environment of Ga, Al and In atoms decreases their accepting ability. The study of an oxidation mechanism of the synthesized complexes by atmospheric oxygen has shown their lower oxidability as compared to original metal trialkyls. Solutions of the complexes are oxidized by atmospheric oxygen with the formation of mixtures of complexes of phosphineoxides with Et₃Ga, Et₂GaOEt and (EtO)₃Ga.

4. Experimental

NMR spectra (in CDCl₃ or C₆D₆) were recorded on a Bruker AM-360 spectrometer.

Table 5
Bond lengths (Å) and angles (°) for Ph₃P:MEt₃ (**7b,d,f**).

Bond length/Å or angle (°)	Compound		
	7b M = Al	7d M = Ga	7f M = In
M(1)–C(5)	1.9764(13)	1.9915(12)	2.183(2)
M(1)–C(1)	1.9790(11)	1.9883(15)	2.184(2)
M(1)–C(3)	1.9792(13)	1.9946(15)	2.189(2)
M(1)–P(1)	2.5413(4)	2.5375(3)	2.7453(5)
P(1)–C(19)	1.8165(10)	1.8173(12)	1.820(2)
P(1)–C(7)	1.8211(10)	1.8226(12)	1.820(2)
P(1)–C(13)	1.8241(10)	1.8221(12)	1.823(2)
C(5)–M(1)–C(1)	116.97(6)	116.50(6)	120.04(8)
C(5)–M(1)–C(3)	114.05(7)	114.83(6)	115.52(8)
C(1)–M(1)–C(3)	114.42(5)	114.71(8)	114.68(8)
C(5)–M(1)–P(1)	101.73(4)	104.81(4)	99.715(5)
C(1)–M(1)–P(1)	105.13(4)	101.76(5)	100.56(6)
C(3)–M(1)–P(1)	101.85(4)	101.33(4)	101.27(5)

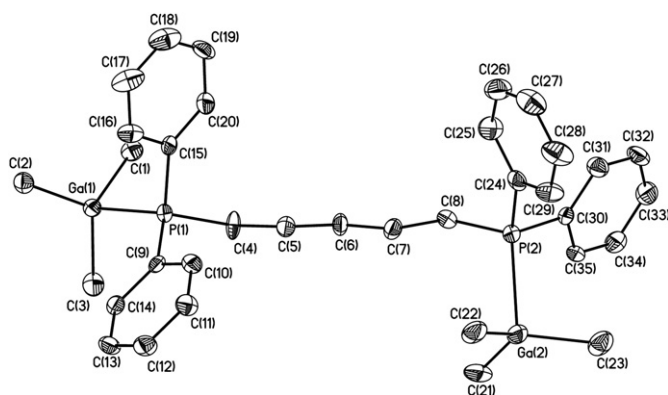


Fig. 13. Molecular structure of compound 9c.

Table 6
Bond lengths (Å) and angles (°) for Ph₂P(CH₂)₃PPh₂:2MMe₃ (**8a,c,e**).

Bond length/Å or angle (°)	Compound		
	8a M = Al	8c M = Ga	8e M = In
M(1)–C(1)	1.9800(16)	1.9929(16)	2.181(2)
M(1)–C(2)	1.9810(16)	1.9991(15)	2.189(2)
M(1)–C(3)	1.9740(15)	1.9857(15)	2.172(2)
M(1)–P(1)	2.5008(5)	2.5069(4)	2.7043(5)
P(1)–C(4)	1.8353(13)	1.8362(13)	1.8367(19)
P(1)–C(6)	1.8200(12)	1.8184(13)	1.8209(19)
P(1)–C(12)	1.8113(12)	1.8190(12)	1.8171(19)
C(3)–M(1)–C(1)	119.54(7)	115.14(7)	116.08(10)
C(3)–M(1)–C(2)	114.86(7)	119.54(7)	121.14(10)
C(1)–M(1)–C(2)	114.91(7)	115.07(7)	115.92(11)
C(3)–M(1)–P(1)	101.11(5)	100.91(5)	98.73(7)
C(1)–M(1)–P(1)	95.73(5)	105.82(5)	103.97(7)
C(2)–M(1)–P(1)	106.38(5)	95.76(5)	93.82(7)

Mass spectra were recorded on MAT-311A spectrometer using direct input into ion source or a capillary column (30 m, SE-30, 70 eV).

IR spectra were recorded on X-29 spectrophotometer in paraffinic oil.

ICP spectra were recorded on Atom Scan 25 spectrometer manufactured by Thermo Jarrell Ash.

Samples of gallium complexes were thermogravimetrically analyzed on EXSTAR TG/DTA7000 derivatograph manufactured by SII Nanotechnology Inc. (heating rate 5 °C/min, argon feed rate 1 l/min).

4.1. The analysis of the samples by ICP spectroscopy

The technique is based on decomposition of a sample of an organoelement compound, which is fed to the plasma burner in the argon flow, in a high-temperature zone of the plasma discharge.

Radiation from excited atoms and ions goes to the monochromator, where after decomposed on the diffraction grating it is registered by photomultiplier tubes which convert optical signals into electric ones with a value in direct proportion to radiation intensity.

3A Group organometallic compounds are taken to the sampler in the atmosphere of dry inert gas (nitrogen or argon). In the atmosphere of dry inert gas (nitrogen or argon) the sample is dissolved in dry freshly distilled diglyme to form an adduct. A homogenized sample solution cooled to room temperature is injected directly to the plasma of the device. The concentration of impurities in the sample is calculated with allowance for the dilution factor. This technique of taking and preparing samples rules out a loss of volatile impurities in the analyzed sample.

Table 7
Bond lengths (Å) and angles (°) for Ph₂P(CH₂)₃PPh₂:2MeT₃ (**8b,d,f**).

Bond length/Å or angle (°)	Compound		
	8b M = Al	8d M = Ga	8f M = In
M(1)–P(1)	2.5300(5)	2.5238(5)	2.7468(6)
M(1)–C(1)	1.9918(15)	1.9932(18)	2.204(2)
M(1)–C(3)	1.9886(16)	1.9978(15)	2.199(2)
M(1)–C(5)	1.9830(14)	1.9927(16)	2.192(2)
P(1)–C(9)	1.8336(12)	1.8383(15)	1.825(2)
P(1)–C(15)	1.8210(12)	1.8069(15)	1.825(2)
P(1)–C(7)	1.8200(12)	1.8152(16)	1.837(2)
C(5)–M(1)–C(1)	115.32(7)	114.28(7)	121.72(9)
C(5)–M(1)–C(3)	115.69(6)	113.45(7)	113.58(9)
C(1)–M(1)–C(3)	114.45(7)	118.85(8)	115.87(9)
C(5)–M(1)–P(1)	102.47(4)	98.06(5)	100.01(7)
C(1)–M(1)–P(1)	96.21(4)	106.05(7)	92.80(6)
C(3)–M(1)–P(1)	109.90(5)	102.71(5)	107.59(7)

Table 8
Bond lengths (Å) and angles (°) for Ph₂P(CH₂)₅PPh₂:2GaMe₃ (**9c**).

Ga(1)–C(1)	1.987(4)	C(1)–Ga(1)–C(3)	113.03(17)
Ga(1)–C(3)	1.989(4)	C(1)–Ga(1)–C(2)	117.39(17)
Ga(1)–C(2)	1.995(4)	C(3)–Ga(1)–C(2)	118.95(16)
Ga(1)–P(1)	2.496(2)	C(1)–Ga(1)–P(1)	96.46(13)
Ga(2)–C(22)	1.985(4)	C(3)–Ga(1)–P(1)	103.96(14)
Ga(2)–C(21)	1.985(4)	C(2)–Ga(1)–P(1)	102.33(11)
Ga(2)–C(23)	1.986(4)	C(22)–Ga(2)–C(21)	114.58(17)
Ga(2)–P(2)	2.527(3)	C(22)–Ga(2)–C(23)	118.18(17)
P(2)–C(24)	1.813(4)	C(21)–Ga(2)–C(23)	116.80(18)
P(2)–C(30)	1.820(4)	C(22)–Ga(2)–P(2)	103.36(11)
P(2)–C(8)	1.826(4)	C(21)–Ga(2)–P(2)	99.32(12)
P(1)–C(15)	1.817(4)	C(23)–Ga(2)–P(2)	99.94(14)
P(1)–C(4)	1.822(4)		
P(1)–C(9)	1.823(4)		

4.2. X-ray diffraction analysis

X-ray diffraction analyses of compounds 7–9 were performed on Bruker SMART APEX II CCD diffractometer ($\lambda[\text{MoK}\alpha] = 0.71073 \text{ \AA}$, ω -scanning). The structures were identified by a direct method and refined by a least square method in anisotropic full matrix approximation on F_{hkl}^2 . Hydrogen atoms were localized from differences of Fourier synthesis of electron density and refined in isotopic approximation by a riding model. Crystallographic data and refinement parameters are given in Table 12. Compounds **8a–c,e,f** and **9c** crystallized with solvate benzene molecules located in channels between molecules of the complexes. All calculations were made using SHELXTL PLUS [34].

All quantum chemical calculations were carried out using the Gaussian 03 software [35]. Optimization of atomic positions was carried out using PBE0 hybrid functional and 6-311G(d,p) basis set. Calculated structures of isolated molecules were tested on stability by calculation of vibrational frequencies. Zero point and counterpoise corrections were taken into account for calculation of M–P bond energies.

All processes went in dry nitrogen or argon. The solvents used were boiled under argon and distilled over LiAlH₄.

Prior to synthesis, phosphines recrystallized from benzene, then their melt was vacuumized for 2 h at 100 °C and residual pressure of 1 Torr.

4.3. Gallium trichloride

Gallium trichloride was synthesized in a quartz thick-walled reactor (diameter 100 mm, height 1000 mm) by passing 5 mol% excess gaseous chlorine through a metal gallium melt. A yield of gallium exceeded 99% as compared with a metal gallium. Its purity was over 99.999% according to ICP spectra. The content of trace impurities in the product is given in Table 1. To transform a crystalline highly hygroscopic product into a bulk material suitable for further preparation of accurately weighed substances as well as solutions, GaCl₃ melt was added by drops into liquid nitrogen. Depending on the rate of introduction of the melt into the refrigerant some granules with diameter of 2–3 mm suitable for further application were obtained.

4.4. Triethylgallium (**5b**)

36.5 g (1.5 mol) of dry magnesium and 330 ml of absolute diethyl ether were loaded under dry nitrogen into a three-necked 0.5 l flask equipped with a reflux condenser, a magnetic stirrer and a drop funnel. The drop funnel was filled with 174.2 g (1.6 mol) of freshly distilled ethyl bromide. After the whole quantity of EtBr was

Table 9
NMR changes of $\Delta\delta_{\text{H}}$ and $\Delta\delta_{\text{P}}$ shifts for phosphines and metal trialkyls during complexation.

No.	Compound	$\Delta\delta_{\text{H}}$					$\Delta\delta_{\text{P}}$
		CH ₂ -M	CH ₃	CH ₂ -P	CH ₂ -C-M	CH ₂ -central	
7a	Ph ₃ P·AlMe ₃	–	+0.42	–	–	–	+0.95
7b	Ph ₃ P·AlEt ₃	+0.25	+0.16	–	–	–	+0.99
7c	Ph ₃ P·GaMe ₃	–	+0.39	–	–	–	+0.99
7d	Ph ₃ P·GaEt ₃	+0.39	+0.29	–	–	–	+1.90
7e	Ph ₃ P·InMe ₃	–	+0.42	–	–	–	–0.46
7f	Ph ₃ P·InEt ₃	+0.46	+0.23	–	–	–	+0.13
8a	(CH ₂) ₃ (PPh ₂ ·AlMe ₃) ₂	–	+0.40	–0.02	–	–0.18	–0.88
8b	(CH ₂) ₃ (PPh ₂ ·AlEt ₃) ₂	+0.16	–0.03	–0.15	–	–0.15	+2.39
8c	(CH ₂) ₃ (PPh ₂ ·GaMe ₃) ₂	–	+0.18	–0.11	–	–0.02	+5.10
8d	(CH ₂) ₃ (PPh ₂ ·GaEt ₃) ₂	+0.11	+0.09	–0.09	–	–0.12	+5.34
8e	(CH ₂) ₃ (PPh ₂ ·InMe ₃) ₂	–	+0.28	–0.05	–	–0.01	0
8f	(CH ₂) ₃ (PPh ₂ ·InEt ₃) ₂	+0.25	+0.12	–0.04	–	–0.01	+1.82
9a	(CH ₂) ₅ (PPh ₂ ·AlMe ₃) ₂	–	+0.25	–0.03	–0.06	–0.2	+0.53
9b	(CH ₂) ₅ (PPh ₂ ·AlEt ₃) ₂	+0.07	+0.03	+0.05	–0.09	–0.2	+1.95
9c	(CH ₂) ₅ (PPh ₂ ·GaMe ₃) ₂	–	+0.30	–0.01	–0.08	–0.22	+2.09
9d	(CH ₂) ₅ (PPh ₂ ·GaEt ₃) ₂	+0.30	+0.28	+0.02	–0.08	–0.22	+3.21
9f	(CH ₂) ₅ (PPh ₂ ·InEt ₃) ₂	+0.38	+0.19	+0.05	–0.04	–0.17	+1.60

* $\Delta\delta = \delta_{\text{компл}} - \delta_{\text{исч}}$. And is a difference of values of chemical shifts of related atoms between complexes and initial metal trialkyl or ligand. A positive $\Delta\delta$ value corresponds to a downfield shift.

added by drops into the flask, the mixture was boiled and stirred for 2 h. Then the drop funnel was filled with 1) 19 ml; 2) 20.9 ml; 3) 23.3 ml; 4) 23.9 ml; 5) 24.6 ml; 6) 25.4 ml; 7) 26.2 ml of 17.9 M solution of GaCl₃ in Et₂O respectively. The solution was added by drops to the Grignard reagent maintaining a moderate boiling of the mixture. After the adding stopped, the mixture was intensively boiled and stirred for 1 h, the solvent was distilled to vapor temperature of 45 °C, then the mixture of the product and ether was condensed into the flask cooled with liquid nitrogen as residual pressure gradually decreased from 150 to 0.1 Torr. The resultant mixture was then separated at a packed refluxer selecting the end fraction in a temperature range 135–144 °C. We obtained 1) 67.55 g; 2) 67.70 g; 3) 67.69 g; 4) 67.75 g; 5) 67.76 g; 6) 61.97 g; 7) 55.09 g of GaEt₃ respectively. Based on ¹H NMR spectra taken without a solvent (in C₆D₆), the end product contained 4% w/w of diethyl ether that was indicated by a quadruplet resonance of O–CH₂ fragments in the area of 4.09 ppm. Fragments of methylene groups bound to the metal atom are characterized by a quadruplet with δ 0.99 ppm, with methyl groups characterized by a triplet with δ 1.53 ppm.

4.5. Rectification of triethylgallium (**5b**)

Triethylgallium that was obtained as described above and contained 4–5% w/w diethyl ether was initially rectified on a packed rectification column (height 300 mm, diameter 20 mm) with a stainless steel prism helix (3 × 3 × 0.2 mm; height of transfer unit

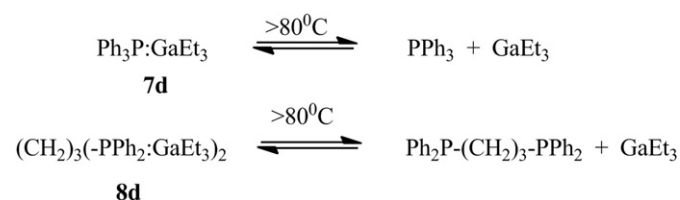
Table 10
Selected structural and thermodynamic parameters of compounds (**7**)–(**9**) according to quantum chemical calculations (PBE0/6-311G(d,p)).

Compound	M–P, Å	M–C	D _e , kcal/mol	ΔH	ΔG
7a	2.577	1.990	15.9	–9.5	–5.6
7b	2.592	1.999	14.9	–9.4	–6.2
7c	2.590	2.210	12.4	–9.1	–4.5
7d	2.592	2.000	14.9	–9.4	–6.2
7e	2.606	2.010	10.0	–9.3	–4.2
7f	2.820	2.223	10.4	–9.5	–6.8
8a	2.561	1.990	16.3	–1.9	–18.6
8b	2.589	1.999	15.1	–1.7	–19.5
8c	2.801	2.207	12.9	–1.4	–16.7
8d	2.574	1.997	15.8	–0.9	–12.4
8e	2.590	1.999	11.5	–1.2	–11.5
8f	2.813	2.221	11.2	–1.1	–6.3

26 mm). The column still was filled with 2.7 kg of GaEt₃. A distillate with vapor temperature of 34–120 °C and 70% w/w ether was collected as the first fraction (8–10% w/w of the total quantity loaded). A distillate with vapor temperature of 120–142 °C and ether content of ca. 10,000 ppm was collected as the second fraction (8–10% w/w of the total quantity loaded). The end fraction was collected at vapor temperatures of 142–143 °C with ether content of ca. 1000 ppm (75–77% w/w of the total quantity loaded). After fractionating was performed on a similar 500 mm high rectification column, with the end fraction collected at vapor temperature 143–144 °C with ether content of ca. 40 ppm (80% w/w of the total quantity loaded). After multiple rectifications of the predistillates collected an aggregate yield of triethylgallium with ether content of ca. 40 ppm was 88–90% of the total quantity of the technical product loaded. Using NMR spectroscopy and chromatomass spectrometry, some triethylgallium, ethyldigalliumhydride, ethoxydiethylgallium and triethoxygallium (see above) were detected in the distillation residue in the rectification column; and the ¹H NMR spectra of the end GaEt₃ showed resonances of ethylene protons with δ 5.76 ppm and ethane protons with δ 0.7 ppm that were identified by their comparison to spectra of reference patterns of hydrocarbon solutions in triethylgallium. The ethylene content in the end product varied from 9 to 54 ppm, with the ethane content varying from 3 to 10 ppm. In order to completely eliminate gas impurities, the product was vacuumized without heating and then bubbled with inert gas.

4.6. Bis-(diphenylphosphine)alkanes (**1,2**)

A 2 l four-necked flask equipped with an effective condenser, a stirrer and a dropping funnel was filled with 500 ml of dry THF which was then deoxygenated for 1 h by transmitting of dry nitrogen. Then 100 g (0.382 mol) of triphenylphosphine was added,



Scheme 10. Isolation of GaEt₃ from complexes **7d** and **8d**.

Table 11

The yield of metal trialkyls in reversible complexation of adducts with 5 mol% phosphines followed by vacuumization at 1 Torr.

Adduct	Temperature, °C		Yield of metal trialkyls, %					
	Of initial decomposition	Of intense decomposition	AlMe ₃	AlEt ₃	GaMe ₃	GaEt ₃	InMe ₃	InEt ₃
7a	100	120–130	84	–	–	–	–	–
7b	90	130–140	–	53	–	–	–	–
7c	80	100–110	–	–	88	–	–	–
7d	80	120–125	–	–	–	90	–	–
7e	80	110–135	–	–	–	–	75	–
7f	85	125–140	–	–	–	–	–	60
8a	95	120–140	86	–	–	–	–	–
8b	85	120–140	–	58	–	–	–	–
8c	80	110–120	–	–	90	–	–	–
8d	80	120–143	–	–	–	93	–	–
8e	85	110–135	–	–	–	–	81	–
8f	85	125–140	–	–	–	–	–	65
9a	95	120–140	80	–	–	–	–	–
9b	85	120–140	–	62	–	–	–	–
9c	80	110–120	–	–	88	–	–	–
9d	80	120–143	–	–	–	92	–	–
9f	85	120–135	–	–	–	–	–	66

and the mixture was stirred till a clear solution was obtained, wherein 6 g (0.856 mol) of freshly prepared ultra-fine lithium flushed with THF was added a little at a time in high purity argon current. The addition rate of the lithium was limited by keeping an

exothermic reaction temperature below 50 °C. When the loading of the lithium was completed, the resultant crimson solution was cooled to 0 °C, and a solution of 50 g (0.442 mol) of 1,3-dichloropropane or 62.3 g (0.442 mol) of 1,5-dichloropentane in 50 ml of

Table 12

Crystallographic data and experimental parameters.

	7a	7b	7c	7d	7e	7f
Empirical formula	C ₂₁ H ₂₄ AlP	C ₂₄ H ₃₀ AlP	C ₂₁ H ₂₄ GaP	C ₂₄ H ₃₀ GaP	C ₂₁ H ₂₄ InP	C ₄₈ H ₆₀ In ₂ P ₂
Formula weight	334.3759	376.43	377.09	419.17	422.19	928.54
Space group	R-3	P2 ₁ /c	R-3	P2 ₁ /n	R-3	P2 ₁ /n
Z	6	4	6	4	6	4
a, Å	14.2841(4)	9.1558(8)	14.299(2)	9.1469(3)	14.357(1)	18.7019(15)
b, Å	14.284(1)	7.9386(7)	14.299(2)	7.9313(2)	14.357(1)	7.9926(6)
c, Å	16.4034(4)	30.197(3)	16.273(2)	30.1382(9)	16.387(1)	30.080(2)
β, °	90.00	94.061(2)	90.00	93.9950(10)	90.00	93.3330(10)
V, Å ³	2898.48(9)	2189.3(3)	2881.2(7)	2181.12(11)	2925.2(1)	4488.7(6)
Density (calc., g cm ⁻³)	1.149	1.142	1.304	1.276	1.438	1.374
μ[Moz] (cm ⁻¹)	1.85	1.71	15.13	13.4	12.91	11.29
F(000)	1068	808	1176	880	1284	1904
2θ _{max} , °	59	60	60	60	107	61
Reflections collected	33,377	27,131	36,275	26,911	108,638	57,719
Independent reflections (R _{int})	1872	6392	1870	6366	8015	13,708
Number of reflections with I > 2σ(I)	1751	5402	1802	5879	6873	11,704
Parameters	82	248	71	246	71	475
R ₁ [I > 2σ(I)]	0.0268	0.0408	0.0193	0.0263	0.0230	0.0286
wR ₂ (all reflections)	0.0791	0.1042	0.0535	0.0616	0.0647	0.0682
Goodness-of-fit	1.007	1.038	0.991	1.019	1.001	1.012
Residual electron density, e·Å ⁻³ (ρ _{min} /ρ _{max})	0.368/–0.199	0.442/–0.285	0.377/–0.345	0.436/–0.432	1.125/–1.373	0.886/–0.688

	8a	8b	8c	8d	8e	8f	9c
Empirical formula	C ₄₅ H ₅₆ Al ₂ P ₂	C ₅₁ H ₆₈ Al ₂ P ₂	C ₄₅ H ₅₆ Ga ₂ P ₂	C ₃₉ H ₅₆ Ga ₂ P ₂	C ₄₅ H ₅₆ In ₂ P ₂	C ₅₁ H ₆₈ In ₂ P ₂	C ₄₁ H ₅₄ Ga ₂ P ₂
Formula weight	712.80	796.95	797.27	726.22	887.47	972.63	748.22
Space group	C2/c	C2/c	C2/c	P4 ₃₁	C2/c	C2/c	P2 ₁ /c
Z	4	4	4	4	4	4	4
a, Å	25.279(2)	25.8405(12)	25.279(2)	9.9767(14)	25.4360(16)	26.024(3)	15.741(15)
b, Å	9.8375(9)	9.8747(4)	9.8375(9)	9.9767(14)	9.9072(6)	9.9407(12)	15.402(14)
c, Å	18.4465(17)	18.7905(8)	18.4465(17)	38.260(6)	18.5576(12)	18.765(2)	18.35(2)
β, °	110.960(2)	105.405(1)	110.960(2)	90.00	110.4780(10)	105.313(2)	114.29(2)
V, Å ³	4283.8(7)	4622.5(3)	4283.8(7)	3808.2(10)	4381.0(5)	4682.1(9)	4055(7)
Density (calc., g cm ⁻³)	1.105	1.145	1.236	1.265	1.345	1.378	1.226
μ[Moz] (cm ⁻¹)	1.71	1.65	13.61	15.23	11.53	10.86	14.33
F(000)	1528	1720	1668	1524	1812	2004	1568
2θ _{max} , °	61	61	61	64	61	60	60
Reflections collected	25120	29614	24826	57649	18986	38363	11771
Independent reflections (R _{int})	6540	7040	6539	6727	6667	6823	11771
Number of reflections with I > 2σ(I)	5252	5487	5724	6262	5691	6103	4300
Parameters	195	249	195	198	192	247	412
R ₁ [I > 2σ(I)]	0.0515	0.0406	0.0346	0.0275	0.0302	0.0350	0.0591
wR ₂ (all reflections)	0.1250	0.1034	0.0899	0.0645	0.0732	0.0992	0.0918
Goodness-of-fit	1.033	1.021	1.014	1.007	1.015	1.000	0.852
Residual electron density, e·Å ⁻³ (ρ _{min} /ρ _{max})	0.841/–0.550	0.475/–0.362	1.045/–0.571	0.463/–0.320	0.928/–0.711	1.939/–1.740	1.168/–0.942

THF was added by drops to the reaction mass with the temperature kept at 0 °C. When dripping was over, the color of the reaction mass turned light-brown. The mixture was boiled at the flask temperature of 80 °C for 3 h. After the mixture got self-cooled to room temperature, 750 ml of deoxygenated methanol was added to it. The mass was cooled to 0 °C, and 125 ml of oxygen-free water was rapidly added by drops into a vigorously stirred mass. The suspension of the deposited diphosphines **1** or **2** was settled at 0 °C for a short time possible, a solution was decanted from them. The residuum was filtered under nitrogen, rinsed with 5 × 25 ml of cold diethyl ether and dried in vacuum for 20 h. Obtained: 21.54 g (yield 35% as compared with Ph₃P) 1,3-bis(diphenylphosphine)propane (**1**) or 29.4 g (yield 35% as compared with Ph₃P) 1,5-bis(diphenylphosphine)pentane (**2**) in the form of white amorphous powders with melting temperatures 61–63 and 41–44 °C respectively that agreed with the literature data [24]. ¹H and ³¹P NMR spectra corresponded to a structure of the compounds and are given in Table 3. When compound **1** was synthesized using not deoxygenated methanol and water, a by process of formation of 1,3-bis(diphenylphosphine)propanemonoxide (**3**) was observed. In this case a mixture of compounds **1** and **3** was a caramel-like, non-crystallizing mass which was subsequently cut by way of fractional recrystallization from the benzene/methanol mixture. Obtained: 8.4 g of compound **1** (yield 13.6%) and 5.2 g of compound **3** (yield 6.36% as compared with Ph₃P) with melting temperatures 121–124 °C. Mass spectra for compound **3** (*m/z*, relative intensity, %): 428 (45) [M]⁺, 351 (100) [M – Ph]⁺, 243(15) [M – Ph₂P]⁺, 229 (11) [Ph₂PO(CH₂)₂]⁺, 227 (6) [M – Ph₂PO]⁺, 215 (34) [Ph₂PO(CH₂)]⁺, 201(48) [Ph₂PO]⁺, 183 (32), 121 (16), 108 (14) [PhP]⁺, 77 (14) [Ph]⁺. Found (%): C 75.60; H 6.07. C₂₇H₂₆OP₂. Calculated (%): C 75.69; H 6.12.

4.7. Purification of triethylgallium by its interaction with aluminum

50 g of triethylgallium obtained as described above with 4.3% w/w of diethyl ether and 1 g of aluminum were stirred for 2 h in the temperature range 100–120 °C. After that 41 g (82%) of Et₃Ga with ether content of ca. 30 ppm was isolated by rectification at boiling temperature 120 °C in small vacuum.

4.8. Purification of triethylgallium by its interaction with gallium trichloride

50 g of triethylgallium obtained as described above with 4.3% w/w of diethyl ether and 1.88 g of gallium trichloride were stirred for

2 h in the temperature range 100–120 °C. After that 44 g (88%) of GaEt₃ with ether content of ca. 25 ppm was isolated by rectification at reduced pressure.

4.9. Synthesis of adducts of trialkyl derivatives of Group 13A metals with aromatic phosphines and diphosphines in benzene

Liquid metal trialkyls **4a,b**, **5a,b**, and **6b** or powder **6a** (a sample was loaded in a nitrogen box with 10 ml of benzene added) in accurately measured quantity of ca. 0.1 mol were loaded using a doser from a cylinder into a four-necked 250 ml flask equipped with a thermometer, a magnetic stirrer and a metal trialkyl feeder connected to a volume doser and a vacuum system, a dropping funnel with back pressure. A quantity of Ph₃P equimole to that loaded or a quantity of diphosphines **1** or **2** which is half the equimole one was prepared as described above, dissolved in 40 ml of benzene and placed in the dropping funnel. The benzene solution of phosphines was added by drops to metal trialkyls for 30 min. The reaction masses were slightly heated. After the adding was over, the reaction masses were stirred for 1 h till they reached a room temperature. While stirred, the reaction masses were vacuumized to isolate benzene at still temperature of at least 5–7 °C until a crystalline phase started to occur, but not more than 25 ml, and were further kept at atmospheric pressure under inert gas for 6–120 h (for complexes **7–8**) or 1–2 months in a dark place (for low-melting complexes **9**) at 10 °C. Deposits of resultant complexes **7–9** were filtered in a nitrogen box. Yields (based on the isolated crystalline phase), melting temperatures and elemental analysis data of the resultant compounds are summarized in Table 13.

4.10. Reversible complexation of metal trialkyls **4–6** with triphenylphosphine and alkanediphosphines **1** and **2**

Ca. 0.1 mol of metal trialkyls **4–6** was treated with diethyl ether to 4% w/w and then added while stirring to 5 mol% excess triphenylphosphine or 0.55 equivalent of diphosphines **1** or **2**. As the exothermic reaction was over, the mixture was vacuumized at 70 °C for 10 h at 1 Torr to eliminate ether, and then the resultant complexes **7–9** were decomposed by means of increased temperature for 2–3 h. Temperature conditions and yields of metal trialkyls are given in Table 11. NMR and mass spectra have not detected diethyl ether in the end product.

Table 13
Yield, melting temperature and elemental analysis data of synthesized complexes **7–9**.

Compound	Yield, %	<i>T</i> _{melt} , °C	Found, %		Formula	Calculated, %	
			C	H		C	H
7a	72	128–130	75.11	7.12	C ₂₁ H ₂₄ AlP	75.43	7.23
7b	62	85–88	76.08	7.98	C ₂₄ H ₃₀ AlP	76.57	8.03
7c	75	133–135	66.78	6.35	C ₂₁ H ₂₄ GaP	66.9	6.41
7d	55	88–89	68.57	7.13	C ₂₄ H ₃₀ GaP	68.77	7.21
7e	68	130–133	59.2	5.69	C ₂₁ H ₂₄ InP	59.7	5.73
7f	42	84–87	61.74	6.43	C ₂₄ H ₃₀ InP	62.09	6.51
8a	77	82–84	75.43	7.88	C ₃₃ H ₄₄ Al ₂ P ₂ · 2C ₆ H ₆	75.82	7.92
8b	73	75–77	76.51	8.52	C ₃₉ H ₅₆ Al ₂ P ₂ · 2C ₆ H ₆	76.86	8.60
8c	90	80–83	67.32	6.95	C ₃₃ H ₄₄ Ga ₂ P ₂ · 2C ₆ H ₆	67.70	7.01
8d	67	73–76	64.23	7.69	C ₃₉ H ₅₆ Ga ₂ P ₂	64.50	7.77
8e	65	70–75	60.13	6.15	C ₃₃ H ₄₄ In ₂ P ₂ · 2C ₆ H ₆	60.83	6.35
8f	40	50–55	62.34	6.93	C ₃₉ H ₅₆ In ₂ P ₂ · 2C ₆ H ₆	62.98	7.05
9a	33	43–45	71.65	8.17	C ₃₅ H ₄₈ Al ₂ P ₂	71.90	8.27
9b	20	28–32	73.22	8.89	C ₄₁ H ₆₀ Al ₂ P ₂	73.63	9.04
9c	26	40–43	67.80	7.21	C ₃₅ H ₄₈ Ga ₂ P ₂ · 2C ₆ H ₆	68.31	7.32
9d	28	27–30	64.98	7.94	C ₄₁ H ₆₀ Ga ₂ P ₂	65.28	8.02
9f	11	26–29	58.11	7.09	C ₄₁ H ₆₀ In ₂ P ₂	58.31	7.16

Acknowledgments

This research was financially supported by JSC Alkyl. We also thank A. Blokhina at JSC Alkyl for her assistance and help in translation of this paper into English.

Appendix A. Supplementary material

The supplementary crystallographic data for this paper was submitted to Cambridge Crystallographic Data Centre (CCDC 770900–770912). These data can be obtained free of charge via www.ccdc.cam.ac.uk/data_request/cif.

References

- [1] B. Gerald, G.B. Stringfellow, *Organometallic Vapour Phase Epitaxy: Theory, Practice*, second ed. Academic Press., London, 1999.
- [2] G.B. Stringfellow, *Epitaxy*, Rep. Prog. Phys. 45 (1982) 469.
- [3] A.C. Jones, P. O'Brien, *CVD of Compound Semiconductors: Precursor Synthesis, Development and Applications*. Weinheim, New York, Basel, Cambridge, Tokyo, 1997.
- [4] K.M. Coward, A.C. Jones, M.E. Pemble, S.A. Rushworth, L.M. Smith, T. Martin, *J. Electronic Mater.* 29 (2000) 151.
- [5] A Kuczkowski, S. Schulz, M. Nieger, *Appl. Organometal. Chem.* 18 (2004) 244.
- [6] R.A. Baldwin, H. Rahbarnoohi, L.J. Jones III, A.T. McPhail, R.L. Wells, P.S. White, A.L. Rheingold, G.P.A. Yap, *Heteroatom. Chem.* 7 (1996) 409.
- [7] M.A. Banks, O.T. Beachley Junior, J.D. Maloney, R.D. Rogers, *Polyhedron* 9 (1990) 335.
- [8] A.H. Cowley, C.S. King, A. Decken, *Organometallics* 14 (1995) 20.
- [9] V.I. Bregadze, L.M. Golubinskaya, L.G. Tonoyan, B.I. Kozyrkin, B.G. Gribov, *Dokl. Akad. Nauk USSR* 212 (1970) 880.
- [10] V.I. Bregadze, L.M. Golubinskaya, B.I. Kozyrkin, *J. Cluster Sci.* 13 (2002) 631.
- [11] D.C. Bradley, H. Chudzynska, M.M. Factor, D.M. Frigo, M.B. Hursthouse, B. Hussain, L.M. Smith, *Polyhedron* 7 (1988) 1289.
- [12] D.C. Bradley, H.M. Dawes, M.B. Hursthouse, L.M. Smith, M. Thornton-Pett, *Polyhedron* 9 (1990) 343.
- [13] V.V. Shatunov, A.V. Lebedev, V.D. Sheludyakov, B.I. Kozyrkin, V.Yu. Orlov, *Khim. Prom. Segodnya* 11 (2009) 27.
- [14] Yu. Rokhov, D. Kherd, R. Lewis, *The Chemistry of Metalorganic Compounds*. Moscow: Publishing House of Foreign Literature, 1963.
- [15] J.J. Byers, W.T. Pennington, G.H. Robinson, *Crystallogr. Sect. C: Cryst. Struct. Commun.* 48 (1992) 2023.
- [16] J.E. Park, J. B-Bae, K. Lee, J.T. Park, H.Y. Chang, M.-G. Choi, *Organometallics* 19 (2000) 5107.
- [17] S.J. Obrey, S.G. Bott, A.R. Barron, *J. Organomet. Chem.* 643 (2002) 53.
- [18] G.E. Coats, *J. Chem. Soc.* (2003) 1951.
- [19] D.A. Atwood, R.A. Jones, A.H. Cowley, S.G. Bott, J.L. Atwood, *Polyhedron* 10 (1999) 1897.
- [20] H. Schumann, U. Hartmann, W. Wassermann, A. Dietrich, F.H. Görlitz, L. Pohl, M. Hostalek, *Chem. Ber.* 123 (1990) 2093.
- [21] P. Jutzi, M. Bangel, B. Neumann, H.-G. Stammel, *Organometallics* 15 (1996) 4559.
- [22] C.H. Lake, S.J. Schauer, L.K. Krannich, C.L. Watkins, *Polyhedron* 18 (1999) 879.
- [23] Y. Zhang, P.H.M. Budzelaar, J.M.M. Smits, R. Gelder, P.R. Hageman, A.W. Gal, *Eur. J. Inorg. Chem.* (2003) 656–665.
- [24] A.M. Bradford, D.C. Bradley, M.B. Hursthouse, M. Motevalli, *Organometallics* 11 (1992) 111.
- [25] C.T. Sirimanne, J.E. Knox, M.J. Heeg, H.B. Schlegel, C.H. Winter, *J. Am. Chem. Soc.* 125 (2003) 11152.
- [26] J.B. Hill, S.J. Eng, W.T. Pennington, G.H. Robinson, *J. Organomet. Chem.* 445 (1993) 11.
- [27] J.-C. Poulin, T.-P. Dang, H.B. Kagan, *J. Organomet. Chem.* 84 (1975) 87.
- [28] P.W. Clark, *J. Organomet. Chem.* 137 (1977) 235.
- [29] G.W. Luther III, G. Beyerle, *Inorg. Synth.* 17 (1977) 186.
- [30] C.A. Tolman, *Chem. Rev.* 77 (1977) 313.
- [31] A.R. Barron, *J. Chem. Soc. Dalton Trans.* (1988) 3047.
- [32] R.D. Shannon, *Acta Crystallogr.* A32 (1976) 751.
- [33] A. Haaland, *Angew. Chem. Int. Ed.* 28 (1989) 992.
- [34] G.M. Sheldrick, *SHELXTL*, Version 5.10. Bruker-AXS Inc, Madison, WI-53719, USA, 1997.
- [35] M.J. Frisch, G.W. Trucks, H.B. Schlegel, G.E. Scuseria, M.A. Robb, J.R. Cheeseman, J.A. Montgomery, Jr., T. Vreven, K.N. Kudin, J.C. Burant, J.M. Millam, S.S. Iyengar, J. Tomasi, V. Barone, B. Mennucci, M. Cossi, G. Scalmani, N. Rega, G.A. Petersson, H. Nakatsuji, M. Hada, M. Ehara, K. Toyota, R. Fukuda, J. Hasegawa, M. Ishida, T. Nakajima, Y. Honda, O. Kitao, H. Nakai, M. Klene, X. Li, J.E. Knox, H.P. Hratchian, J.B. Cross, V. Bakken, C. Adamo, J. Jaramillo, R. Gomperts, R.E. Stratmann, O. Yazyev, A. J. Austin, R. Cammi, C. Pomelli, J.W. Ochterski, P.Y. Ayala, K. Morokuma, G.A. Voth, P. Salvador, J.J. Dannenberg, V.G. Zakrzewski, S. Dapprich, A.D. Daniels, M.C. Strain, O. Farkas, D.K. Malick, A.D. Rabuck, K. Raghavachari, J.B. Foresman, J.V. Ortiz, Q. Cui, A.G. Baboul, S. Clifford, J. Cio-slowski, B. B. Stefanov, G. Liu, A. Liashenko, P. Piskorz, I. Komaromi, R.L. Martin, D.J. Fox, T. Keith, M.A. Al-Laham, C.Y. Peng, A. Nanayakkara, M. Challacombe, P.M.W. Gill, B. Johnson, W. Chen, M.W. Wong, C. Gonzalez, J.A. Pople, Gaussian, Inc., Wallingford CT, 2004.